# 3D URANS Analysis of a Vertical Axis Wind Turbine in Skewed Flows

A. Orlandi[a,b], M. Collu[a], S. Zanforlin[b], A. Shires[c]

[a] *Offshore Renewable Energy Engineering Centre, Cranfield University, Cranfield, MK43 0AL, UK*
[b] *Dipartimento di Ingegneria dell'Energia, dei Sistemi, del Territorio e delle Costruzioni, Universita di Pisa, Pisa 56122, Italy*
[c] *School of Mechanical Engineering, University of Leeds, Leeds LS2 9JT, UK*

**Abstract**

The article demonstrates the potential of an unsteady RANS 3D approach to predict the effects of skewed winds on the performance of an H-type vertical-axis wind turbine (VAWT). The approach is validated through a comparison between numerical and experimental results for a full-scale Darrieus turbine, demonstrating an improved prediction ability of 3D CFD with respect to both 2D CFD and semi-empirical models based on the double multiple stream tubes method. A 3D URANS approach is then adopted to investigate the power increase observed for a straight-bladed small-scale turbine in a wind tunnel when the rotational axis is inclined from 0° to 15° from the vertical. The main advantage of this approach is a more realistic description of complex three-dimensional flow characteristics, such as dynamic stall, and the opportunity to derive local blade flow conditions on any blade portion during upwind and downwind paths. Consequently, in addition to deriving the turbine overall performance in terms of power coefficient, a better insight into the temporal and spatial evolution of the physical mechanisms is obtained. Our principal finding is that the power gain in skewed flows is obtained during the downwind phase of the revolution as the end part of the blade is less disturbed by the wake generated during the upwind phase.

*Keywords:* vertical axis wind turbine, offshore, skewed flow, dynamic stall, CFD

## 1. Introduction

The pursuit of reducing the cost of offshore wind energy in deep waters has led to a re-emerging interest in vertical-axis wind turbines (VAWTs) for floating applications due to apparent advantages over conventional horizontal-axis wind turbines (HAWTs) [1, 2, 3]. In parallel, there is a resurgence of interest in VAWTs as a promising alternative to HAWTs also for small-scale electric power in urban areas [4].

VAWTs are characterised by some significant advantages: the ability to capture wind from any direction without a yaw control mechanism, low noise, compact design, simpler

*Email address:* maurizio.collu@cranfield.ac.uk (M. Collu )

access, installation, maintenance and repair (since the gearbox and drive train components can be located at ground level rather than at the top of the tower as for HAWTs).

Furthermore, although VAWTs generally have a lower aerodynamic efficiency, there is some evidence that VAWTs can be positioned closer together in a wind farm giving a higher power density due to lower wake interference. Furthermore, counter-rotating VAWTs in close proximity have been shown experimentally [5] and numerically [3] to have a mutually beneficial effect on power production.

It is perhaps the offshore environment that has attracted the greatest interest for VAWTs because of several inherent attributes that offer advantages with respect to HAWTs, particularly the scalability and low over-turning moments with better accessibility to drive train components [6, 7].

A correct prediction of the turbine performance in skewed flows is very important for both micro generation in the built environment and large-scale offshore applications [8], since urban winds have noticeable vertical components (micro generation), and waves and unsteady wind speeds will induce pitch/roll motions to the turbine axis and therefore a periodic tilt angle with respect to the vertical (offshore floating wind turbine). HAWTs and VAWTs exhibit completely different behaviours in skewed flows. Theoretical studies and experimental measurements have shown that the power output in a skewed flow is reduced for an HAWT [9]. This trend is mainly due to a reduction in the effective swept area (i.e. the area perpendicular to the oncoming wind direction). Consequently, initial studies have indicated that HAWTs can suffer severe performance losses when installed on floating support structures [10]. On the other hand for VAWTs, depending on the configuration, the performance degradation due to skewed flow is generally lower and for H-VAWT (VAWT with two vertical blades connected to the central tower through one/more arms) configurations the power coefficient may even be enhanced. Experimental investigations on H-VAWT turbines have demonstrated an enhanced performance for relatively small tilt angles (up to $25^\circ - 30^\circ$) depending on the shape of the rotor, whereas a reduced performance is produced by higher skew values [11]. This benefit might be explained by the fact that VAWT blades sweep out a cylindrical surface, as opposed to a planar surface for HAWTs. As a consequence, during misaligned flow operations, the swept area of the turbine is increased.

To account for skewed flow effects on VAWT performance, the efforts of researchers have focused on the implementation of semi-empirical corrections in blade element momentum models [12, 13]. To the authors' knowledge, there are no studies in the literature presenting a 3D CFD (Computational Fluid Dynamics) study on inclined VAWT performance. The present study is aimed at contributing to a better understanding of the physical processes that result in the measured performance enhancement reported for VAWTs in skewed flows.

## 2. Numerical approach

The two wind turbine configurations analysed in this work are:

- the SANDIA 17m-diameter Darrieus-Type VAWT - used to validate the CFD modelling approach that has been adopted. It has an aspect ratio (height to diameter ratio)

equal to 1.02, two blades with a NACA 0015 aerofoil section and a constant chord of 0.612 m. Rotational speed is fixed at 38.7 $RPM$ (rotational speed, in revolutions per minute) for aerodynamic force measurements and 42.2 $RPM$ for $c_p$ measurements [14];

- a two bladed H-Darrieus VAWT with NACA 0018 aerofoil sections and constant 0.08 m chord. The rotor height is 0.5 m and diameter is 0.755 m. This configuration was used in wind tunnel tests to study the influence of skewed flows [4] allowing direct comparison with CFD predictions.

For all the simulations, two different grid levels have been adopted: a fixed sub-grid with the external dimensions of the flow domain, and a dynamic sub-grid that includes the VAWT geometry and allows a relative motion with respect to the fixed grid. This grid arrangement utilises the sliding mesh technique [15] and allows the simulation of the rotating motion of the wind turbine with a steady RANS (Reynolds-averaged Navier-Stokes equations) or URANS (unsteady RANS) analysis.

The CFD process was validated for the SANDIA National Labs configuration using both 2D and 3D grids. The 2D mesh adopted is a hybrid structured-unstructured mesh with around 460 000 elements. The flow domain external dimensions were $37D$ x $25D$, and the wall distance from the first layer of cells is set at 1.6*10-5$c$ with $y+$ (dimensionless wall distance) $< 1$, where $D$ is the diameter of the turbine and $c$ is the blade chord length. The 3D grid contains around 2 800 000 elements with flow domain external dimensions of $15D$ x $5D$ x $4D$ and a wall distance equal to 1.9*10-4$c$, resulting in $y+ < 5$.

For the analysis of the rotor in a skewed flow, only a 3D approach was considered and the mesh contains around 1 800 000 elements. The external dimensions are $14D$ x $30D$ x $12D$ and the wall distance is 1*10-4c, necessary for an averaged y+ $< 5$, following a mesh sensitivity analysis performed in order to verify if the grids adopted were sufficiently fine to resolve the primary flow features. Figure 1 shows the analysis for the 2D model for the 17m Darrieus VAWT and the 3D model for the small H-Darrieus VAWT; the 3D model of the SANDIA turbine has been excluded from this analysis due to the high number of cells of the domain, but the mesh adopted is similar to that used by Howell [16] and Zhang [17].

The CFD software used for the present analyses is FLUENT v.15, developed by Ansys Inc. This study is based on the URANS implicit model, and turbulence is modelled using the k-$\omega$ SST (Shear Stress Transport) model. This turbulence scheme was adopted because of its aptitude in cases involving high adverse pressure gradients and therefore smooth surface separations [18]. The air was considered as incompressible since the different cases studied did not exceed a local Mach number greater than 0.3.

## 3. Results

### *3.1. Verification of the CFD model*

This paper focuses on two wind speed operating conditions: $TSR = 4.6$ (Tip Speed Ratio) (low-wind speed case) and $TSR = 2.33$ (high wind speed case), for the SANDIA 17m-diameter test case. Since chordwise pressures for this case were measured at the equatorial

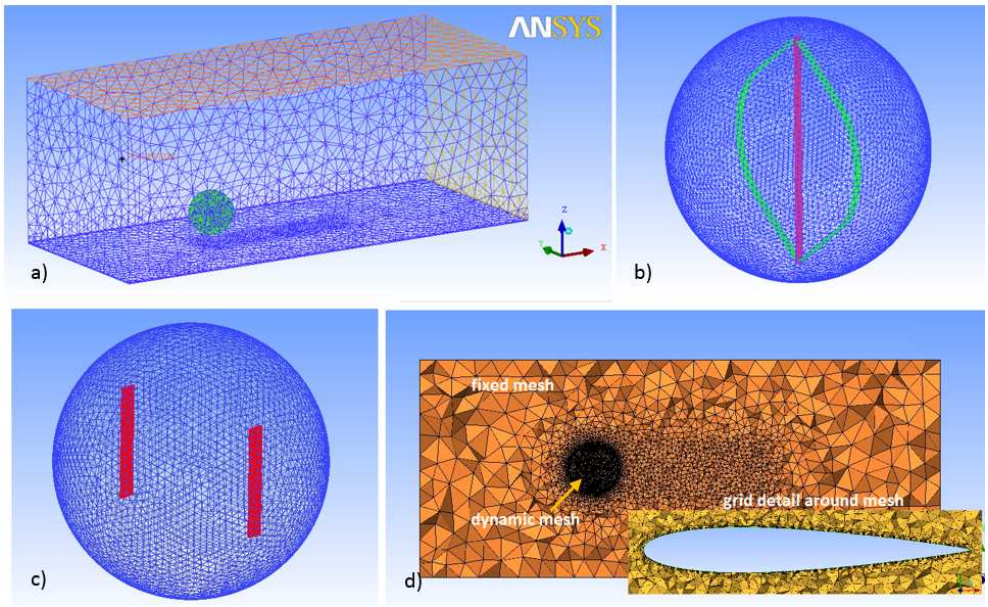


Figure 1: (a) External domain, (b) details of 3D grid for SANDIA 17m Darrieus-Type wind turbine, and (c) of the H-Darrieus Type Wind Turbine, (d) volume mesh

station of the turbine blade, it is expected that the local flow at this station is 2D and therefore that 2D CFD simulations give a good approximation of the flow. Normal and tangential force coefficients were obtained by integrating the chordwise pressure distributions as reported by Akins [14]. The normal and tangential force coefficients $c_n$ and $c_t$ are defined as:

$$c_n = \frac{F_n}{\frac{1}{2}\rho U_\infty^2 c} \tag{1}$$

$$c_t = \frac{F_t}{\frac{1}{2}\rho U_\infty^2 c} \tag{2}$$

where $F_n$ and $F_n$ are, respectively, the normal and tangential force on the blade per unit of span [N], $\rho$ is the air density [kg/m$^3$], and $U_\infty$ is the free stream wind velocity [m/s].

Predicted normal and tangential force coefficients from both 2D and 3D CFD simulations are compared against the experimental data in Figure 2 (equatorial plane of the rotor). The azimuthal angle of the blade $\theta$ is measured such that $\theta = 0°$ at the beginning of the upwind path. These figures show good agreement between the 2D and 3D CFD models and the experimental data. The shapes of the normal and tangential force coefficient curves reproduce the measured trends well from a qualitative point of view, though there are some differences in peak values at corresponding azimuthal angles.

As would be expected, the predicted normal force coefficient data are in closer agreement with measured data than the tangential force coefficient data, with a maximum relative difference of 15% over the upwind cycle of the revolution ($70° < \theta < 130°$), whilst for the

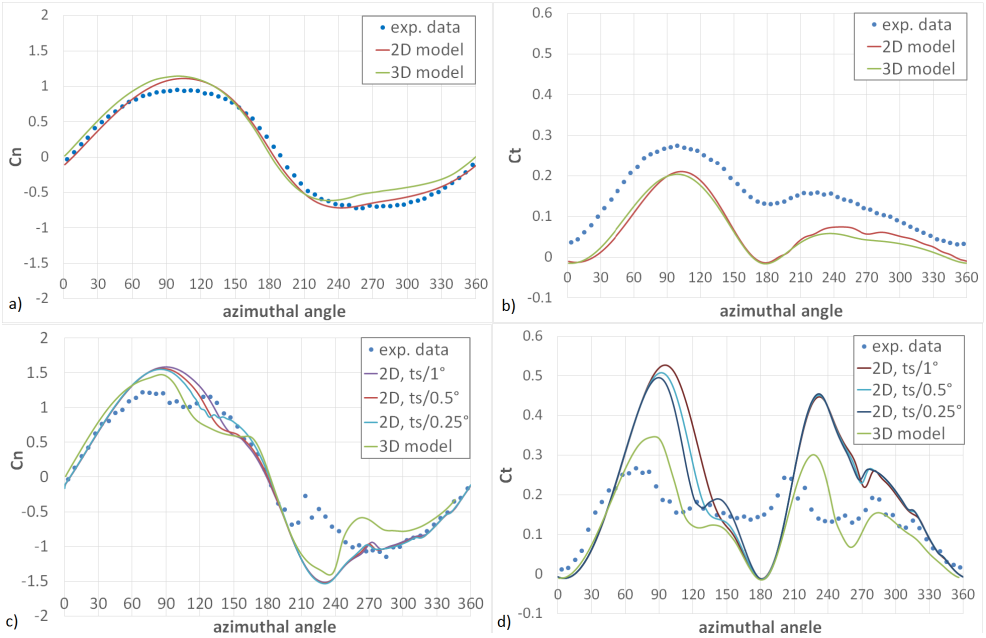


Figure 2: Normal force coefficient and tangential force coefficient, calculated at $TSR$=4.6 (a,b) and at $TSR$=2.33 (c,d)

downwind cycle any differences (with the 2D predicted data) are small. Both 2D and 3D CFD models underestimate the tangential force coefficient at all blade positions, resulting in a maximum relative difference of ∼55% over the downwind cycle.

Figures 2c and 2d show 2D CFD results obtained using different time steps to assess how they affect results at the higher wind-speed condition ($TSR = 2.33$), where flow separations and dynamic stall can influence performance. Because of these more complex and dynamic features, a time-step sensitivity analysis was performed using; 1°, 0.5° and 0.25° of azimuthal angle for each time step. Generally, the 2D simulation tends to over-predict tangential and normal force coefficients at this flow condition. Measured data at this condition indicate that flow separates and subsequently reattaches on the blade surface between 80° and 130° blade azimuth positions, with a potential increase in both the normal and tangential force coefficients due to dynamic stall over the final quarter of both upwind and downwind cycles. The CFD models give good agreement when the flow is attached, but separation appears to be delayed due to a higher blade azimuth angle (and therefore blade angle of attack). Consequently the model overestimates the peak normal force coefficient in the first half of the revolution, with a maximum relative error of ∼28% for the 2D model. If a smaller time-step is adopted, the separation of the flow occurs at a smaller azimuth angle but does not have a significant effect. The CFD models also predict a delay in the occurrence of stall over the downwind cycle, resulting in a big difference with experimental data. The 3D model gives a better prediction of the flow behaviour and of the aerodynamic forces on the blade, particularly in terms of tangential force coefficient. One advantage of the 3D approach could be a better estimation of dynamic stall and also lag effects due to the unsteady flow. The

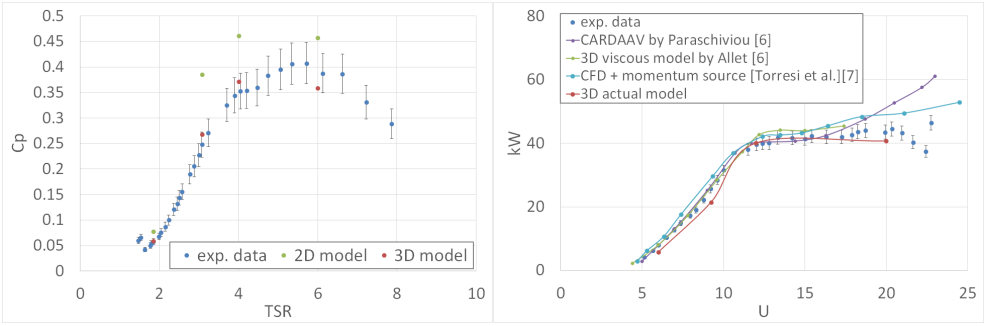


Figure 3: $c_p$ and power curve as function of *TSR*

2D CFD models cannot fully describe the complex dynamics of the flow whilst the 3D CFD model can take into account the near and far field flow developments surrounding the real geometry of the wind turbine, as also shown by Howell [16].

Figure 3 compares the predicted and measured coefficient of power ($c_p$) and power production curves for the SANDIA 17m Darrieus turbine. $C_p$ is defined as:

$$C_p = \frac{Power}{\frac{1}{2}\rho U_\infty^3 DH} \tag{3}$$

where $H$ is the blade height [m]. Due to the better prediction of the tangential force coefficient at higher wind speeds, the 3D CFD results are in closer agreement with experimental data and are generally within 10%. The 2D CFD model over-predicts power at high wind speeds, as would be expected from the previous analysis. Figure 3 also compares the data with those predicted using BEM (Blade Element-Momentum) approaches by Allet [19] as well as another CFD approach [20]. The advantage of the CFD approach becomes clearer at high wind-speed conditions, where greater accuracy in predicted power is achieved.

### *3.2. Rotor in skewed flow*

Since the purpose of this work is to determine the influence of changes to the inclination of a VAWTs' rotational axis relative to the flow direction on the rotor performances, a 3D CFD model is necessary. The two bladed H-Darrieus VAWT configuration was used, with measured wind tunnel test data available for a straight and inclined rotor [4]. A preliminary analysis in order to assess the best turbulence model scheme was performed for this wind turbine, without skewed inflow. This analysis considered two of the most referenced turbulence models for cases including strong adverse pressure gradients: k-$\epsilon$ RNG (Re-Normalisation Group) and k-$\omega$ SST. The comparison was based on the calculation of the power coefficient $C_p$ at different values of *TSR*.

Figure 4 shows good agreement of the k-$\omega$ SST model with wind tunnel test data, though the k-$\epsilon$ RNG scheme gives poor results, particularly at low wind speeds. The difference between the k-$\omega$ SST model and the measured data is within 10%, except at the highest wind speed. This difference between these two models can be attributed to an overproduction

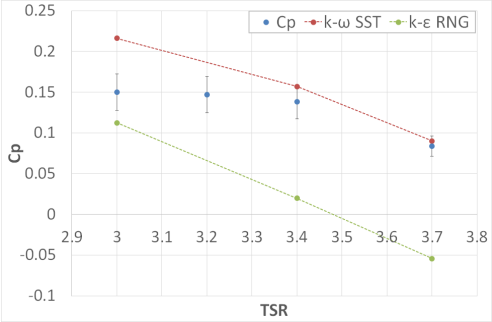


Figure 4: $c_p$ curve for the H-Darrieus experimental wind turbine. Experimental data from wind tunnel test by Mertens [4]

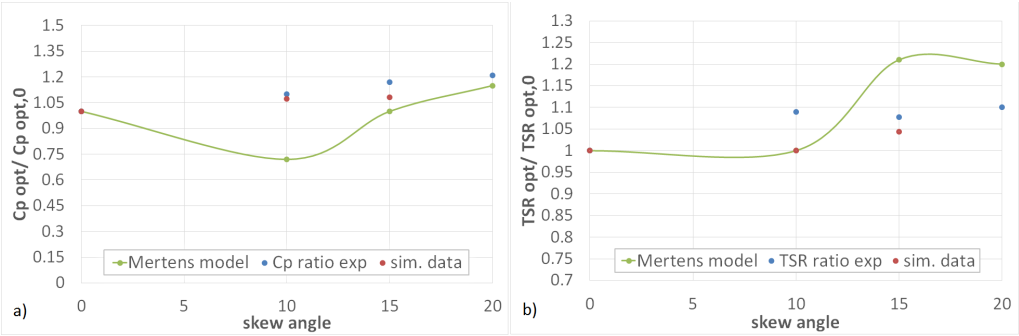


Figure 5: $c_p$ ratio and $TSR$ ratio for H-Darrius Turbine at different tilt angles. The ratios refer to the maximum values of the variables reached at different tilt angles normalized by the maximum value calculated at 0 tilt angle. From wind tunnel test by Mertens [4]

in wall shear stresses by the fully-turbulent k-$\epsilon$ RNG model, which led to a smaller averaged torque value.

Both test cases have demonstrated that the k-$\omega$ SST model can simulate the power production of a VAWT with reasonable accuracy. Consequently, the k-$\omega$ SST turbulence model was adopted for quasi-static simulations of the rotating H-VAWT configuration at fixed inclination or tilt angles. The inclination angle $\Phi$ was varied in 5° increments from 5° to 15°. Higher inclination angles were not considered since it is assumed that the H-VAWT is installed on an offshore floating platform and these structures are designed not to exceed a limit of ±15° oscillations about the vertical axis [8].

Figure 5a refers to the ratio of the maximum value of $c_p$ at different tilt angles normalized by the maximum value at 0° skew angle; figure 5b refers to the ratio of $TSR$ at which the maximum $c_p$ is reached at different values of $\Phi$, normalized by the maximum value at $\Phi = 0$. The CFD results are also compared with measured wind tunnel results and results from a BEM model developed by Mertens [4]. The BEM model under-predicts the power in a skewed flow, while the CFD results are in good agreement with the wind tunnel measurements.

This means that the present model can well describe the behaviour of the flow acting on the blade sections, such as the rise of dynamic stall and the effects of the wake generated

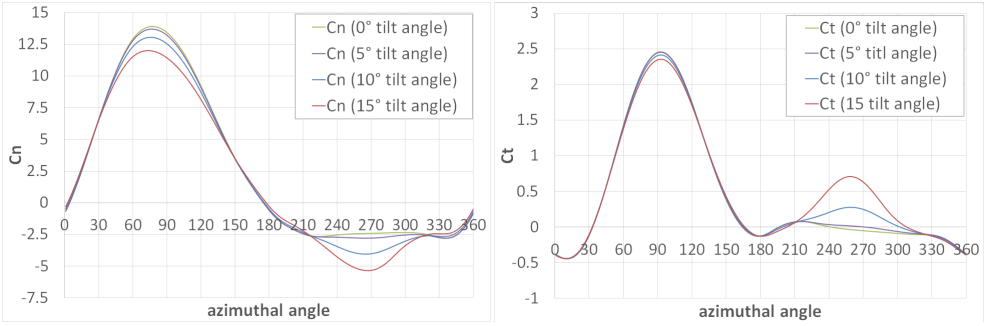


Figure 6: Normal force and tangential force coefficient as a function of the azimuthal angle, at different tilt angles

by the previous blade on the oncoming one. The comparison also reveals that the Mertens model does not agree very well with the experimental data. The main reason is due to the DMST (Double-Multiple Stream Tube) model not including the semi-empirical corrections that account for the dynamic stall. Indeed, this consideration is linked to the results shown in Figure 5b. It is evident that, at a higher *TSR* ratio, which implies higher rotational velocity of the wind turbine (since the inlet velocity is fixed at 7m/s), and at higher tilt angles, the $c_p$ ratio values are closer to the one obtained in the wind tunnel tests corresponding to the same tilt angle. The combined effects of the increased rotational velocity and the augmentation of the tilt angle lead to a smaller influence of the dynamic stall and so a better matching between the Mertens model and experimental data. However, also shown in this graph, the present model matches the *TSR* ratio measurements better than the Mertens model.

As seen from figure 5, the $c_p$ increases with $\Phi$ due to the increases of the blade tangential force coefficient. The normal and tangential force coefficients predicted at the equatorial plane of the rotor are shown in Figures 6a and 6b respectively. As regards the normal forces, small changes are seen in the first half of the revolution, where the maximum difference between the cases at $\Phi = 0°$ and $\Phi = 15°$ is equal to 1.8%, while downwind the blade experiences normal forces that increase with tilt angle.

Regarding the tangential force coefficient, which has a direct impact on the rotor torque and power, although slightly reduced values are experienced over the upwind cycle (maximum of 4.5% lower than the case at $\Phi = 0°$), significant increases are experienced over the downwind cycle. Consequently this increase in the tangential force coefficient is the reason for the augmentation of the normalised power. In fact, figure 6 shows that the maximum value of $c_n$ and Ct is reached for the case at $\Phi = 15°$:

$$\frac{c_{n,MAX\{180°<\theta<360°\},\Phi=15°}}{c_{n,MAX\{180°<\theta<360°\},\Phi=0°}} = 2.32 \quad \frac{c_{t,MAX\{180°<\theta<360°\},\Phi=15°}}{c_{t,MAX\{180°<\theta<360°\},\Phi=0°}} = 7.1 \tag{4}$$

This beneficial effect is because the bottom part of the rotor in the downwind section is less influenced by the passage of the previous blade, i.e. less wake interference. This is shown in figure 8, showing colour shaded velocity contours on a plane parallel to the flow direction.

During the revolution, the wind over the upwind cycle is decelerated by the passage of

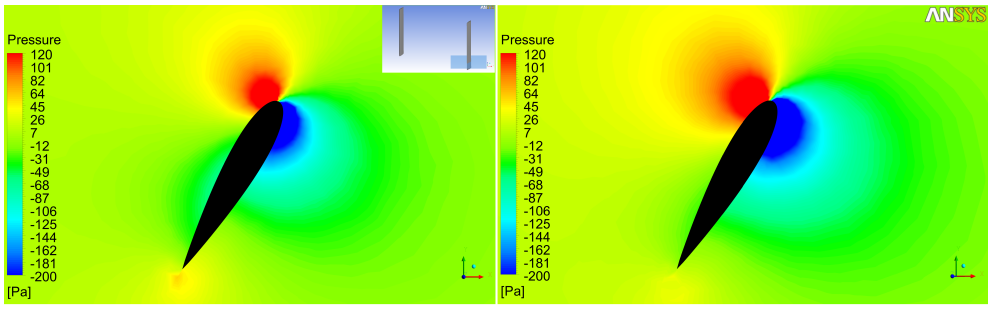


Figure 7: Pressure field calculated at $\Phi = 0°$ (left) and $\Phi = 15°$ (right), considering a blade section at 0.25m distant from the tip in the less influenced zone

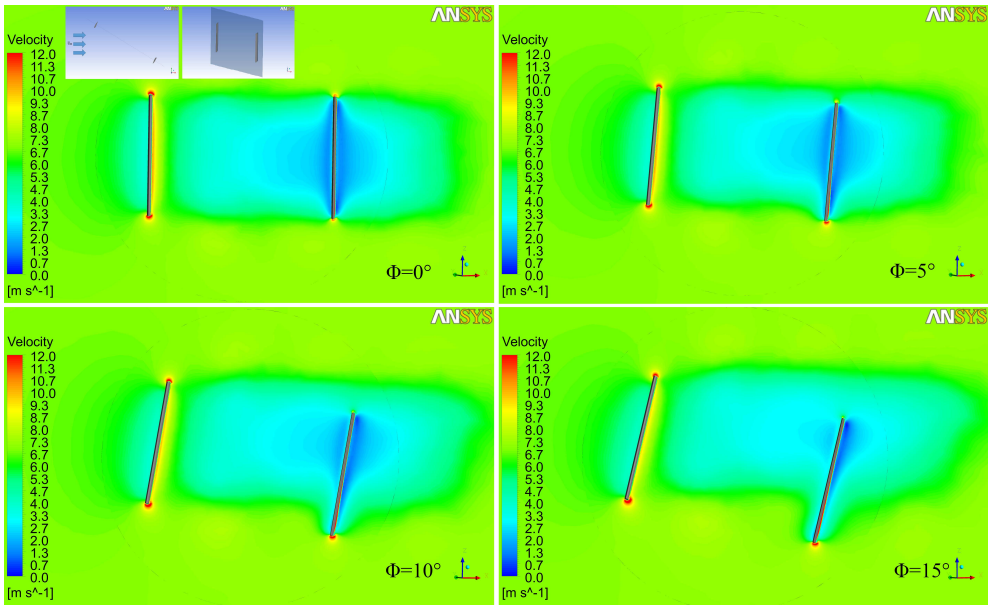


Figure 8: Velocity field at different tilt angle

the blades, i.e. there is a momentum loss associated with the work extracted by the rotor. This wake moves downstream in the wind direction creating a zone of low momentum flow that is crossed by the advancing blade. When the rotor is not inclined to the flow, the entire downwind blade encounters the wake from the upwind blade. However, at different $\Phi$ a lower part of the blade is outside of this wake and thus experiences a higher dynamic pressure and an increase in local aerodynamic forces.

Similarly, figure 9 shows the effect of the wake from the passage of the preceding blade on the downwind cycle in terms of vorticity contours, and highlights that at higher tilt angles the vorticity is reduced in this region.

The static pressure field is shown in Figure 7 for a blade aerofoil section at $\theta = 240°$ and at a distance of 0.25m from the lower blade tip (i.e. far enough to be not influenced by the tip vortices). This qualitative comparison shows some significant differences in the local pressure field as the rotor is tilted to $\Phi = 15°$, especially on the suction surface, resulting in

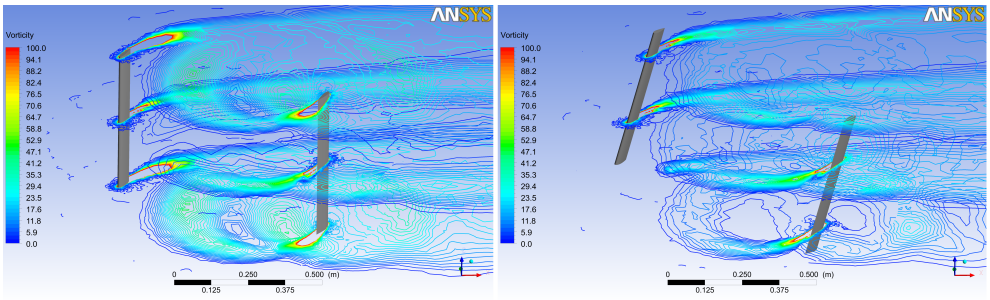


Figure 9: Vorticity contours at $\Phi = 0°$ (left) and $\Phi = 15°$ (right)

a higher value of lift and an augmentation in the power coefficient.

## 4. Conclusions

It has been shown that the CFD simulations using a URANS model are a promising way to investigate the complex phenomena that are present in an analysis of a VAWT. After initially validating the CFD model, the second part of the paper utilizes the method to consider the performance increments that have been observed in skewed flow. The 3D CFD model shows better prediction of the behaviour of the fluid, which involves unsteady three-dimensional effects such as dynamic stall. However, some differences from the experimental data have been displayed and it could be useful to investigate these further using more complex models, LES (Large Eddy Simulation) or DES (Detached Eddy Simulation) models for example, in order to give a more precise description of these dynamic phenomena. As regards the analysis of an H-VAWT in different tower tilting conditions, a quasi-static analysis has been performed, with the aim to separate and analyse the causes that lead to an increase of the coefficient of power $c_p$. The present work offers a possible interpretation of this phenomenon, which was studied through experimental tests and only briefly using a semi-empirical model by Mertens. This study founds that the gain is due to the downwind part of the rotor being less disturbed by the wake generated by the blades in the upwind part. Since the interest in the future use of VAWTs is primarily on floating platforms for offshore applications, it could be interesting to evaluate the influence of real motion on the rotor performances. However, it is important to note that it has been possible to determine and localize the physical mechanisms described above using a relatively simple numerical model, i.e. with only 2.5 millions of cells for a full scale turbine and about 2 million for the small turbine, a relatively simple turbulence model (two-equations model), and appropriate time steps that were found as a good compromise between computational costs and accuracy in results.

## References

[1] M. Borg, A. Shires, M. Collu, Offshore floating vertical axis wind turbines, dynamics modelling state of the art. part i: aerodynamics, Renewable and Sustainable Energy Reviews 39 (2014) 1214–1225.

[2] M. Borg, M. Collu, A comparison between the dynamics of horizontal and vertical axis offshore floating wind turbines, Philosophical Transactions of the Royal Society A: Mathematical, Physical and Engineering Sciences 373 (2035).
[3] S. Giorgetti, G. Pellegrini, S. Zanforlin, Cfd investigation on the aerodynamic interferences between medium-solidity darrieus vertical axis wind turbines, Energy Procedia (accepted).
[4] S. Mertens, Wind energy in urban areas: concentrator effects for wind turbines close to buildings, Refocus 3 (2) (2002) 1–13.
[5] M. Kinzel, Q. Mulligan, J. O. Dabiri, Energy exchange in an array of vertical axis wind turbines, Journal of Turbulence 13 (38) (2012) 1–13.
[6] A. Shires, Design optimisation of an offshore vertical axis wind turbine, Proceedings of the ICE-Energy 166 (1) (2013) 7–18.
[7] M. Borg, A. Shires, M. Collu, Offshore floating vertical axis wind turbines, dynamics modelling state of the art. part i: Aerodynamics, Renewable and Sustainable Energy Reviews 39 (2014) 1214–1225.
[8] M. Collu, M. Borg, A. Shires, N. F. Rizzo, E. Lupi, Flovawt: Further progresses on the development of a coupled model of dynamics for floating offshore vawts, in: Proceedings of the ASME 2014 33rd International Conference on Ocean, Offshore and Arctic Engineering, 8-13 June, 2014, San Francisco, USA, 2014.
[9] C. Tongchitpakdee, S. Benjanirat, L. N. Sankar, Numerical simulation of the aerodynamics of horizontal axis wind turbines under yawed flow conditions, Journal of Solar Energy Engineering 127 (4) (2005) 464–474.
[10] D. Bekiropoulos, R. M. Rieß, T. Lutz, E. Krämer, D. Matha, M. Werner, P. W. Cheng, Simulation of unsteady aerodynamic effects on floating offshore wind turbines, in: 11th German Wind Energy Conference, 7-8 November 2012, Bremen Germany, 2012.
[11] S. Mertens, G. van Kuik, G. van Bussel, Performance of an h-darrieus in the skewed flow on a roof, Journal of Solar Energy Engineering 125 (2003) 443–440.
[12] A. Bianchini, G. Ferrara, L. Ferrari, S. Magnani, An improved model for the performance estimation of an h-darrieus wind turbine in skewed flow, Wind Engineering 36 (6) (2012) 667–686.
[13] H. A. Madsen, M. Barone, B. Roscher, P. Deglaire, I. Arduin, et al., Comparison of aerodynamic models for vertical axis wind turbines, in: Journal of Physics: Conference Series, Vol. 524, IOP Publishing, 2014, p. 012125.
[14] R. E. Akins, Measurement of surface pressure on an operating vertical-axis wind turbine, Tech. Rep. SAND89-7051, SANDIA Nat. Labs (1989).
[15] Ansys, Ansys Fluent 12.0. User's Guide, Ansys Inc. (2009).
[16] R. Howell, N. Qin, J. Edwards, N. Durrani, Wind tunnel and numerical study of a small vertical axis wind turbine, Renewable Energy 35 (2010) 412–422.
[17] L. X. Zhang, Y. B. Liang, X. H. Liu, Q. F. Jiao, J. Guo, Aerodynamic performance prediction of straight-bladed vertical axis wind turbine based on cfd, Advances in Mechanical Engineering 2013.
[18] F. R. Menter, Zonal two equation k-omega model for aerodynamic flows, in: 24th Fluid Dynamics Conference, July 6-9, Orlando, Florida, 1993.
[19] A. Allet, I. Paraschivoiu, Viscous flow and dynamic stall effects on vertical-axis wind turbines, International Journal of Rotating Machinery 2 (1) (1995) 1–14.
[20] M. Torresi, B. Fortunato, S. M. Camporeale, Modello cfd per il calcolo delle prestazioni e degli effetti di scia di turbine eoliche ad asse verticale, La Termotecnica.